

**ENHANCEMENTS TO THE BAYESIAN INFRASOUND
SOURCE LOCATION METHOD**

Omar E. Marcillo, Stephen J. Arrowsmith, Rod W. Whitaker, and Dale N. Anderson

Los Alamos National Laboratory

Sponsored by the National Nuclear Safety Administration

Award No. DE-AC52-06NA25396/LA12-Signal Propagation-NDD02

ABSTRACT

We report on R&D that is enabling enhancements to the Bayesian Infrasound Source Location (BISL) method for infrasound event location. The focus of this effort is on improving BISL through the development and implementation of physics-based priors. Phase identification in BISL is incorporated through a prior probability density function on group velocity. We report on the development of a distance-dependent prior through a massive simulation effort that will be validated by a ground-truth data analysis effort. In addition to providing constraints for the prior Probability Density Function (PDF), this coupled effort is also providing constraints on the probability distributions that are used in the likelihood equations in BISL. We assess the enhancement in location precision using a dynamic prior, instead of the previous uniform prior, for some example events. Finally, we discuss efforts to improve the numerical implementation of BISL using Monte Carlo integration.

Report Documentation Page				Form Approved OMB No. 0704-0188	
Public reporting burden for the collection of information is estimated to average 1 hour per response, including the time for reviewing instructions, searching existing data sources, gathering and maintaining the data needed, and completing and reviewing the collection of information. Send comments regarding this burden estimate or any other aspect of this collection of information, including suggestions for reducing this burden, to Washington Headquarters Services, Directorate for Information Operations and Reports, 1215 Jefferson Davis Highway, Suite 1204, Arlington VA 22202-4302. Respondents should be aware that notwithstanding any other provision of law, no person shall be subject to a penalty for failing to comply with a collection of information if it does not display a currently valid OMB control number.					
1. REPORT DATE SEP 2012		2. REPORT TYPE		3. DATES COVERED 00-00-2012 to 00-00-2012	
4. TITLE AND SUBTITLE Enhancements to the Bayesian Infrasound Source Location Method				5a. CONTRACT NUMBER	
				5b. GRANT NUMBER	
				5c. PROGRAM ELEMENT NUMBER	
6. AUTHOR(S)				5d. PROJECT NUMBER	
				5e. TASK NUMBER	
				5f. WORK UNIT NUMBER	
7. PERFORMING ORGANIZATION NAME(S) AND ADDRESS(ES) Los Alamos National Laboratory,P.O. Box 1663 ,Los Alamos,NM,87545				8. PERFORMING ORGANIZATION REPORT NUMBER	
9. SPONSORING/MONITORING AGENCY NAME(S) AND ADDRESS(ES)				10. SPONSOR/MONITOR'S ACRONYM(S)	
				11. SPONSOR/MONITOR'S REPORT NUMBER(S)	
12. DISTRIBUTION/AVAILABILITY STATEMENT Approved for public release; distribution unlimited					
13. SUPPLEMENTARY NOTES Published in the Proceedings of the 2012 Monitoring Research Review - Ground-Based Nuclear Explosion Monitoring Technologies, 18-20 September 2012, Albuquerque, NM. Volume II. Sponsored by the Air Force Research Laboratory (AFRL) and the National Nuclear Security Administration (NNSA). U.S. Government or Federal Rights License					
14. ABSTRACT We report on R&D that is enabling enhancements to the Bayesian Infrasound Source Location (BISL) method for infrasound event location. The focus of this effort is on improving BISL through the development and implementation of physics-based priors. Phase identification in BISL is incorporated through a prior probability density function on group velocity. We report on the development of a distance-dependent prior through a massive simulation effort that will be validated by a ground-truth data analysis effort. In addition to providing constraints for the prior Probability Density Function (PDF), this coupled effort is also providing constraints on the probability distributions that are used in the likelihood equations in BISL. We assess the enhancement in location precision using a dynamic prior, instead of the previous uniform prior, for some example events. Finally, we discuss efforts to improve the numerical implementation of BISL using Monte Carlo integration.					
15. SUBJECT TERMS					
16. SECURITY CLASSIFICATION OF:			17. LIMITATION OF ABSTRACT Same as Report (SAR)	18. NUMBER OF PAGES 8	19a. NAME OF RESPONSIBLE PERSON
a. REPORT unclassified	b. ABSTRACT unclassified	c. THIS PAGE unclassified			

OBJECTIVES

This research aims to enhance infrasound event localization by utilizing both empirical observations and model-based propagation constraints in the BISL algorithm (Modrak et al., 2010) in the form of prior information.

The specific objectives of this research are discussed below:

Modeling infrasound propagation under a comprehensive set of atmospheric scenarios.

To first order, vertical variations in atmospheric temperatures, wind speeds, and wind directions determine the effective velocity and thus propagation paths at regional and global distances. To capture the variability of acoustic propagation in time and space, multi-year multi-scale atmospheric specification datasets are used to run the numerical modeling with rays propagating at representative directions and elevation angles covering regional and global distances.

Extracting information from modeling, and generating and implementing prior information into BISL.

By modeling infrasound propagation, we can classify ray paths that return to ground with the respective velocities, ranges, and maximum elevation. This information leads to the generation of propagation catalogs that can be used for the generation of prior information that is fed into the localization algorithm to constrain the solution to physically meaningful scenarios.

Estimating accuracy and precision for standard and enhanced prior PDF for BISL implementation.

Measuring the successfulness of the enhanced localization requires the introduction of metrics that account for the precision and accuracy of the solution. The BISL localization algorithm is applied to global and regional ground-truth events to estimate the 95% credibility area and the offset between estimated and real events to assess the precision and the accuracy of the algorithms.

Exploring further enhancements for localization schemes.

Our planned mathematical manipulation of the BISL framework will allow further enhancements by allowing the likelihood density function to probe more complex parameter spaces.

RESEARCH ACCOMPLISHED

Overview of the BISL and Theory of Enhancement.

The BISL method estimates the most likely source location and origin time by performing a grid search over a 4D parameter space (Modrak et al., 2010). This multidimensional space includes the two Cartesian coordinates (x_0 and y_0), velocity (v), and time (t_0). In the Bayesian framework, the posterior probability density function (posterior PDF $P(m | d)$) assesses the probability of a model under certain model parameters ($m \equiv \{x_0, y_0, v, t_0\}$) given a specific dataset ($d \equiv \{t_i, \theta_i\}$ arrival times t_i and back azimuth θ_i) and is written as:

$$P(m | d) = c(d)P(m)P(d | m) \quad (1)$$

Where, $P(m)$ is the prior PDF, $P(d | m)$ the likelihood PDF and $c(d)$ a normalization function. $P(d | m)$ is the joint distribution of the errors in back azimuth $\Theta_i(\theta_i | m)$ and origin time $\Phi_i(\theta_i | m)$ between the data and the forward model evaluated in each point of the parameter space (Modrak et al., 2010):

$$P(d | m) = \prod_{i=1}^n \Theta_i(\theta_i | m) \Phi_i(\theta_i | m) \quad (2)$$

where, n is the number of stations in the network, $\Theta_i(\theta_i | m) = \frac{1}{\sqrt{2\pi\sigma_\theta^2}} \exp\left[-\frac{1}{2}\left(\frac{\gamma_i}{\sigma_\theta}\right)^2\right]$ and

$$\Phi_i(t_i | m) = \frac{1}{\sqrt{2\pi\sigma_\phi^2}} \exp\left[-\frac{1}{2}\left(\frac{\varepsilon_i}{\sigma_\phi}\right)^2\right]$$

the error distribution of back azimuths and arrival times, σ_θ and σ_ϕ

the corresponding variances, $\gamma_i = \theta_i - \tilde{\theta}_i$, $\varepsilon_i = t_i - \tilde{t}_i$, $\tilde{\theta}_i$ and \tilde{t}_i the back azimuth and arrival time at station i of a candidate source of the parameter space. $P(m)$ accounts for potential prior information that can be used to constrain the parameters. The prior distribution can be written as:

$$P(m) = p(x_0, y_0)p(t_0)p(v) \quad (3)$$

Marginalization

The posterior PDF ((1) can be marginalized over any dimension of the parameter space. BISL marginalizes over the velocity (v), and time or origin (t_0) and obtains a new posterior PDF over the probable event location $\{x_0, y_0\}$:

$$\begin{aligned} P(\{x_0, y_0\} | d) &= \int_{t_0, v} c(d)P(m)P(d | m) \\ &= p(x_0, y_0) \int_{t_0, v} p(t_0)p(v)P(d | \{x_0, y_0, t, v\}) \\ &= c'(d)p(x_0, y_0)P(d | \{x_0, y_0\}) \end{aligned} \quad (4)$$

where, $c'(d)$ is the new normalization function. The marginalization process, integration over specific dimensions, allows the assimilation of prior information in the form of the prior PDF ((3). Earlier implementations of BISL (Arrowsmith and Whitaker, 2008) use very basic priors that just constrain upper and lower limits of the sound propagation (0.35 to 0.22 km/s, respectively) and assign flat probabilities to the velocities within this range. This velocity range is selected to assess group velocity of rays refracting in the thermosphere (0.22-0.24 km/s), stratosphere (0.28-0.31 km/s), and troposphere (0.30-0.34 km/s) (Cepelch et al., 1998). The approach taken here is to create prior PDFs for group velocity that assign different probabilities to sub-regions of the 0.22-0.35 km/s interval. By performing numerical simulations of infrasound propagation using a comprehensive set of atmospheric scenarios, we create propagation catalogs that are used to evaluate the probability of occurrence of group velocity for a specific range (r_a), azimuth (ϕ_a), and time (t_a) such that:

$$p(v) = K(v, r_a, \phi_a, t_a) \quad (5)$$

where, K is a function that retrieves and normalizes information from the propagation catalogs such that

$\int_v K(v, r_a, \phi_a, t_a)dv = 1$. Assuming that there is not prior information for the location and time of origin of the event, we can write $p(x_0, y_0)p(t_0) = 1$. Using (5), (3) can be written as:

$$P(m) = K(v, r_a, \phi_a, t_a).$$

Networks (groups of sensor arrays) can have complete or partial azimuthal coverage while recording an event. Networks with arrays located at similar distances and azimuths may see similar atmospheric conditions, and therefore a unique prior PDF can be assigned to them. On the other hand, networks with good azimuthal coverage may see very different atmospheric conditions depending on the highly anisotropic wind field. In the latter case, a

unique prior PDF based on a single azimuth, range, and time is not adequate to provide information to the entire network. Below we discuss future implementations of BISL that will properly account for such scenarios. For now, a more appropriate prior PDF can be formed by averaging the prior PDFs for each array of the network into a general prior PDF:

$$P(m) = k \sum_{i=1}^n K_i(v, r_a, \phi_a, t_a) \quad (6)$$

where, n is the number of arrays in the system, and $k = 1 / \int_v \left(\sum_{i=1}^n K_i \right) dv$ a new normalization coefficient.

Azimuth Dependent Celerity-Range Histograms and Prior PDF Generation.

We generated two propagation catalogs using model-based regional and global atmospheric specifications. Infrasound can propagate at local (few 10s km), regional (100s km), and/or global distances (1000s km). At very local (few kilometers) and local distances, topography and source geometry can play a significant role in propagation. On the other hand, propagation at regional and global distances is mainly driven by the atmospheric structure. These specifications are generated by the NRL-G2S atmospheric model (Drob et al., 2003) and include air temperature, and zonal and meridional wind from the ground to 140 km. The regional dataset comprises atmospheric specifications every 6 hours for eleven years for a location centered at the Utah. The global dataset comprises atmospheric specifications taken within a one-year period for locations randomly distributed around the entire surface of the Earth. Ray tracing uses the tau-p method (Garcés et al., 1998; Drob et al., 2003) for rays launched at azimuths covering 360° in steps of 30°, and elevation angles between 1° and 50° at 2° interval and extending out to 2000km and 12000 km horizontal distance for regional and global catalogs. As a result of these simulations, we extract celerity, maximum elevation, and range for multiple bounces for rays that are refracted to the ground. To display these results, we introduce the Celerity Range Histogram (CRH), which displays the ratio between the number of rays that reach the ground and the number of profiles at specific ranges and celerities. The CRHs use: 1) an evenly discretized range, from 0 to 2000 km and 0 to 10000 km for regional and global catalogs respectively, with 50 km interval, and 2) evenly spaced celerities from 0.2 to 0.35 km/s with 0.01 km/s interval.

As the propagation of acoustic energy is controlled by the highly anisotropic vertical effective velocity profiles, we developed azimuth dependent CRHs by grouping ray-path features in four groups (quadrants) depending on launch azimuth. Quadrants covering 315-45 and 135-225 degrees are used to capture the influence of meridional winds in propagation. The 45-135 and 225-315 quadrants are expected to capture the influence of zonal winds. In order to capture the variability in time of the propagation, mainly related to changes in the stratospheric winds (Whitaker and Mutschlecner, 2008), different CRHs were computed for different parts of the year. Figure 1 shows two regional azimuth dependent CRHs for the summer and winter of 2005. The two main components in the histograms (0.29-0.32 km/s and 0.22-0.26 km/s) correspond to the expected thermospheric and stratospheric returns. Seasonal variability (summer-winter) is noted specially for stratospheric returns at azimuths influenced by zonal winds.

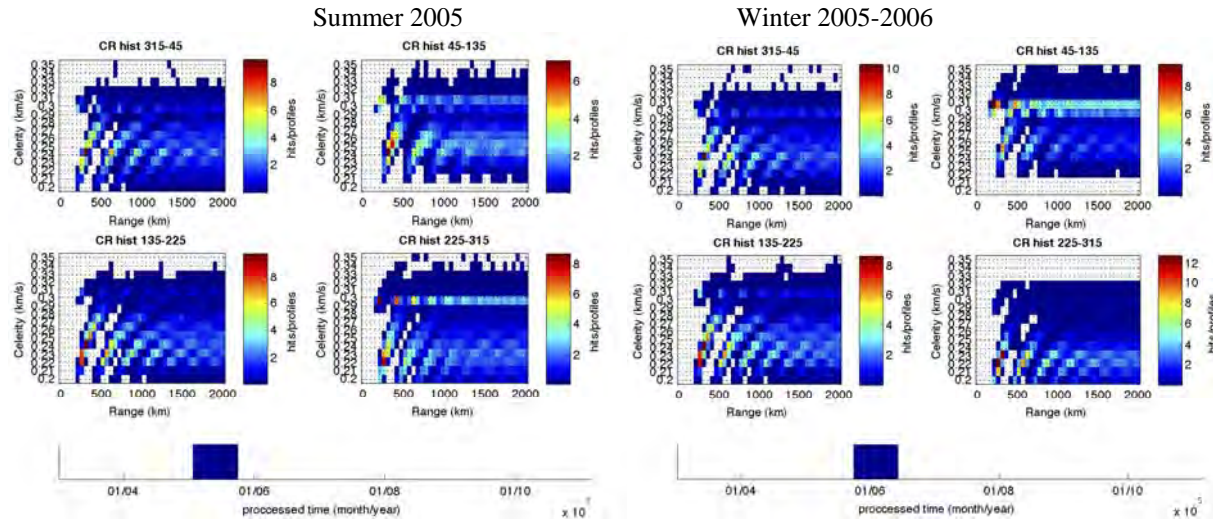


Figure 1. Azimuth dependent Celerity Range Histograms for Winter 2005-2006 (panel a) and Summer 2005 (panel b). CRHs display the ratio (color axis) between the number of rays that return to ground and the associated number of profiles (used in the propagation modeling) at specific celerities (y-axis) and ranges (x-axis).

Figure 2 shows azimuth dependent CRHs for the global catalog. It is interesting to notice that for distances above 1000 km the histograms are very homogenous and seasonal variation is weaker than the effect for regional distances. This effect can be related to the random distribution of the locations used to get the specifications, as the seasonal wind patterns in northern and southern hemispheres have opposite behaviors.

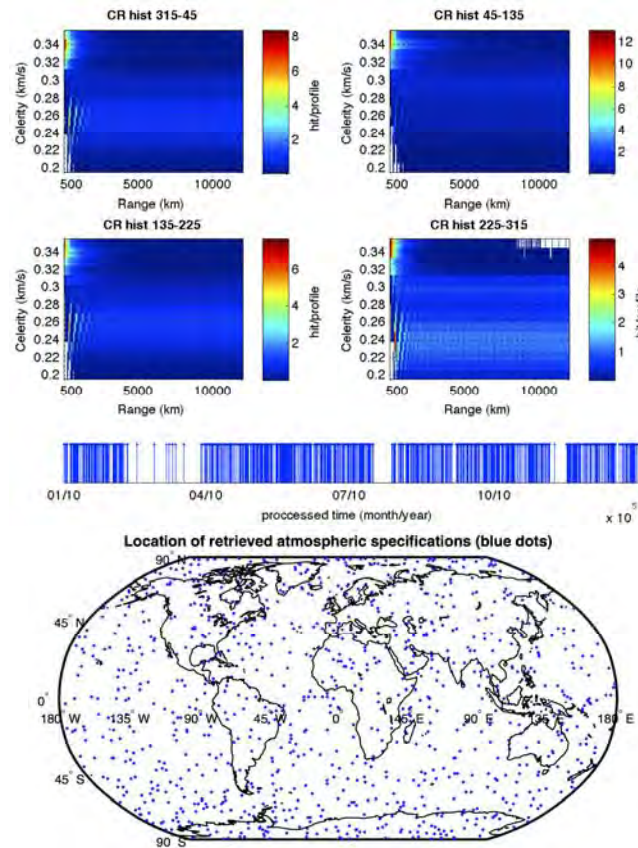


Figure 2. Global azimuth dependent CRH.

Using CRH-based Prior PDF to Enhance BISL.

Every point of the $\{x_0, y_0\}$ parameter sub-space has CRH-based prior PDFs for each element of the network. Station-specific prior PDFs are averaged into one celerity distribution that is used to marginalize the celerity axis. We tested the performance of BISL with both uniform and CRH-based prior PDFs using a surface explosion. This event was a 100-ton ANFO explosion conducted at the Sayarim Military Range, Negev desert in Israel on January 26, 2011 (Gitterman et al., 2011). The event was recorded for three stations of the International Monitoring System (IMS) in I31KZ, I46RU, and I34MN, with distances of up to 6300 km. Figure 3a shows the localization of the detecting IMS stations and Sayarim, this figure also shows the results of using flat and CRH-based prior PDFs for localization using BISL. These results show a significant enhancement in the localization precision (decrease in the 95% credibility area). However, both results display an offset between estimated and actual event location (red star) that can be related to the influence of wind in long-range propagation. In the current implementation of the BISL algorithm back (θ) and launch (ϕ) azimuths correspond geometrically, such that $\theta = \phi + \pi$. However, wind can introduce propagation offsets perpendicular to the launch angle and change the expected back azimuth. We are exploring optimal techniques to correct for this effect.

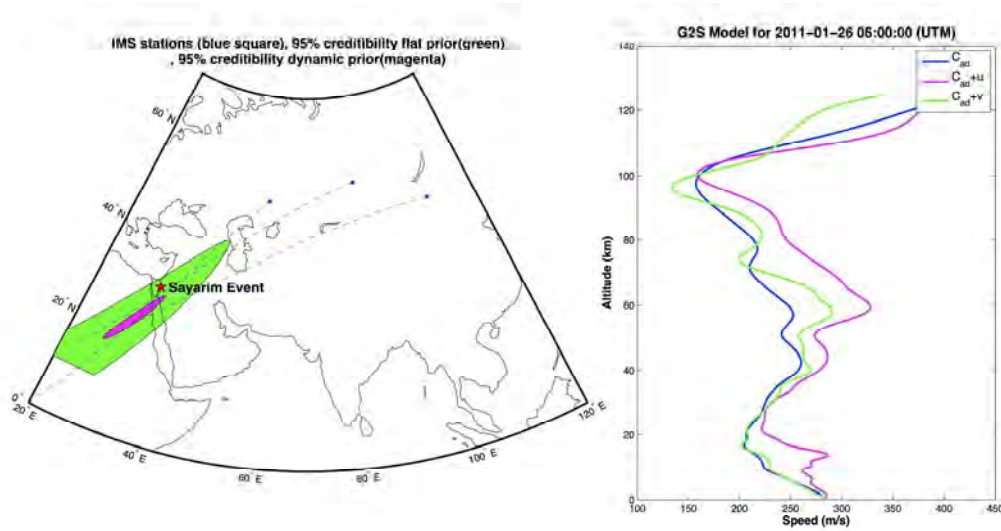


Figure 3. Using uniform and CRH-based prior PDFs for localization using BISL. a) Location of the three stations of the IMS (blue squares) that recorded and identified the Sayarim event (red star), 95% credibility areas using flat (green) and CRH-based (magenta) priors. b) NRL-G2S based atmospheric profiles at the location of the explosion.

Analytical Expression for Model-Based CRH

We are exploring the generation of analytical CRHs based on the decomposition of model-based CRHs. We form vertical cross-sections of an analytical CRH (celerity distributions for specific ranges, azimuths, and times) by linear combination of three probability density functions (PDFs) each characterizing thermospheric (f_H), stratospheric (f_S) and tropospheric (f_T) celerity distributions:

$$\Psi(v, r_a, \phi_a, t_a) = \eta_T f_T(\mu_T, \sigma_T) + \eta_S f_S(\mu_S, \sigma_S) + \eta_H f_H(\mu_H, \sigma_H), \quad (7)$$

where, μ_X and σ_X are mean and standard deviation of an interval X, and η_X a weight coefficient for the same function in (0,1) and the sum of weight functions equal to one. (7) is commonly known as a mixed PDF. This decomposition of elements is intended to provide a physical view of the CRHs, which can be interpreted as the superposition of the three main atmospheric ducts. The parameters and coefficients required for this decomposition are estimated using model-based CRHs. First, the celerity is regrouped in three intervals: 1) 0.22-0.27 km/s,

2) 0.28-0.31 km/s, and 3) 0.30-0.34 km/s. Second, the hit/profile ratios for these new intervals are added, and mean and standard deviation are estimated. These nine parameters (three for each interval) are passed to the (7) to generate Ψ which is the analytic version of K . The function f can have various distribution shapes. We used the normal distribution in this study; however, further analysis should determine the most appropriate shape distribution for f . Figure 4 shows the analytic version of the CRH of Figure 1b. The intensity and width of the thermospheric and stratospheric returns are well recovered in this analytic CRH compared to the model-based one.

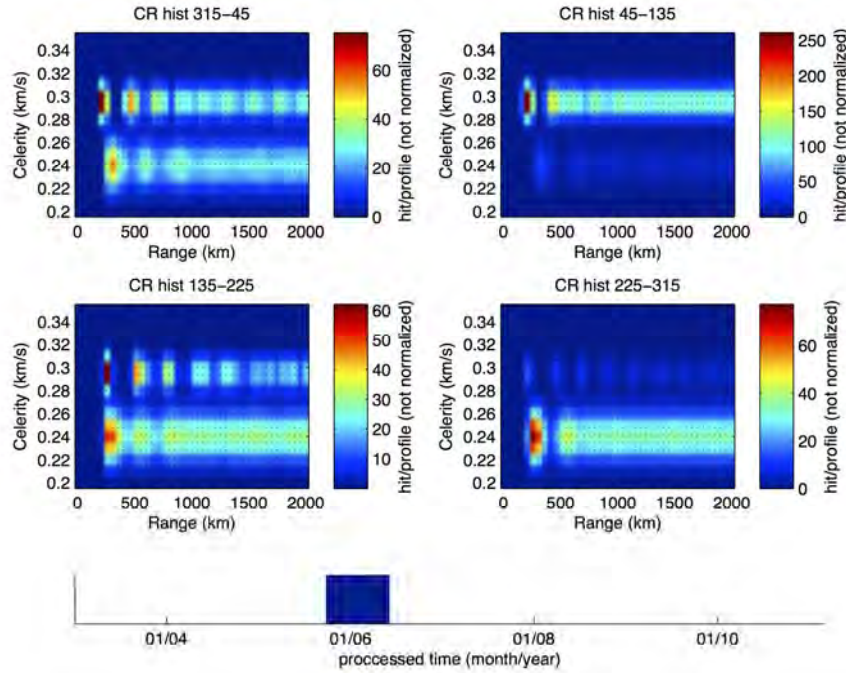


Figure 4. Analytic version of the CRH. This figure is the analytic version of the summer version of the CRH showed in Figure 1.

CONCLUSIONS AND RECOMMENDATIONS

Implementing azimuth and range dependent prior information for group velocity in the BISL algorithm can significantly enhance the precision of event localization. The azimuth dependent CRHs prove to be an effective tool to display and summarize the results of ray propagation modeling. Extracting and normalizing cross-sections of the CRH can easily generate prior PDFs for specific ranges. By using CRH-based prior PDFs we were able to locate an event and determine a 95% confidence area that is significantly smaller than the one using flat priors. Our ongoing research is focused now on studying further enhancements in the application and generation of prior information. Several mathematical representations of the weighting proportions η_x in Equation 7 are under development.

The implementation of the BISL algorithm described here assumes a uniform CRH-based prior PDF for the entire network (averaged version of the array-specific prior PDFs). However, even at regional distances each station of the network has different pictures of the atmosphere between source and receivers. This BISL implementation cannot accommodate for station specific prior information as it sees the network as a whole entity in the 4D parameter space. Further work would require the manipulation of the BISL mathematical framework to include station-specific priors. This work may require probing more complex parameter space that can include expanding the velocity from a parameter to a vector of parameters, with one velocity parameter for each array. This expansion would allow applying array-specific prior PDFs, however, this will increase the dimensions of the parameter space and the corresponding marginalization can slow the application of the algorithm. Our on-going research also includes code development for Monte Carlo integration of the BISL posterior kernel to efficiently probe these more complex spaces and to enable real-time or near real-time applications.

ACKNOWLEDGEMENTS

We would like to acknowledge David Green (AWE Blacknest) and Alexis Le Pichon (CEA) for the helpful discussions that motivated the approach taken in this document.

REFERENCES

- Arrowsmith, S. J. and R. Whitaker (2008). Inframonitor: A tool for regional infrasound monitoring, in *Proceedings of the 2008 Monitoring Research Review Proceedings: Ground-Based Nuclear Explosion Monitoring Technologies*, LA-UR-08-05261, Vol 2, pp. 837–843.
- Cepilecha, Z., J. Borovička, W. Elford, D. ReVelle, R. Hawkes, V. Porubčan, and M. Šimek (1998). Meteor phenomena and bodies. *Space Science Reviews* **84**(3), 327–471.
- Drob, D. P., J. M. Picone, and M. Garcés (2003). Global morphology of infrasound propagation. *J. Geophys. Res.* **108**(D21), 4680.
- Garcés, M. A., R. A. Hansen, and K. G. Lindquist (1998). Traveltimes for infrasonic waves propagating in a stratified atmosphere, *Geophys. J. Int.* **135**(1), 255–263.
- Gitterman, Y., J. Given, J. Coyne, R. Waxler, J. Bonner, L. Zerbo and R. Hofstetter (2011). Large-scale controlled surface explosions at sayarim, israel, at different weather patterns, for infrasound calibration of the international monitoring system. in *Proceedings of the 2011 Monitoring Research Review: Ground-Based Nuclear Explosion Monitoring Technologies*, LA-UR-11-04823, Vol. 2, pp. 766–777.
- Modrak, R. T., S. J. Arrowsmith, and D. N. Anderson (2010). A bayesian framework for infrasound location. *Geophys. J. Int.* **181**(1), 399–405.
- Whitaker, R. W. and J. P. Mutschlecner (2008). A comparison of infrasound signals refracted from stratospheric and thermospheric altitudes. *J. Geophys. Res.* **113**(D8), D08117.